

Migration of surface excitations in highly-excited nanosystems probed by intense resonant XUV radiation

This content has been downloaded from IOPscience. Please scroll down to see the full text.

2015 J. Phys. B: At. Mol. Opt. Phys. 48 244011

(<http://iopscience.iop.org/0953-4075/48/24/244011>)

View [the table of contents for this issue](#), or go to the [journal homepage](#) for more

Download details:

IP Address: 188.61.106.37

This content was downloaded on 21/11/2015 at 12:12

Please note that [terms and conditions apply](#).

Migration of surface excitations in highly-excited nanosystems probed by intense resonant XUV radiation

R Katzy¹, A C LaForge¹, Y Ovcharenko², M Coreno³, M Devetta^{4,12},
M Di Fraia⁵, M Drabbels⁶, P Finetti⁷, V Lyamayev¹, T Mazza⁸, M Mudrich¹,
P O'Keeffe⁹, P Piseri⁴, O Plekan⁷, K C Prince⁷, S Stranges^{10,11}, C Callegari⁷,
T Möller² and F Stienkemeier¹

¹Physikalisches Institut, Universität Freiburg, D-79104 Freiburg, Germany

²Institut für Optik und Atomare Physik, TU Berlin, D-10623 Berlin, Germany

³CNR-Istituto di Struttura della Materia, Basovizza Area Science Park, I-34149 Trieste, Italy

⁴Dipartimento di Fisica & CIMaNa, Università degli Studi di Milano, I-20133 Milano, Italy

⁵Department of Physics, University of Trieste, I-34127 Trieste, Italy

⁶Laboratoire Chimie Physique Moléculaire, Ecole Polytechnique Fédérale de Lausanne, 1015 Lausanne, Switzerland

⁷Elettra-Sincrotrone Trieste, I-34149 Basovizza, Trieste, Italy

⁸European XFEL GmbH, D-22761 Hamburg, Germany

⁹CNR-Istituto di Struttura della Materia, I-00016 Monterotondo Scalo, Italy

¹⁰Department of Chemistry and Drugs Technologies, University Sapienza, I-00185 Rome, Italy

¹¹CNR-IOM Tasc Laboratory, Basovizza, Area Science Park, I-34149, Trieste, Italy

E-mail: aaron.laforge@physik.uni-freiburg.de

Received 2 August 2015, revised 22 September 2015

Accepted for publication 5 October 2015

Published 13 November 2015



CrossMark

Abstract

Ionization dynamics of resonantly excited helium nanodroplets have been studied by intense XUV light. By doping the nanodroplets with atoms that either attach to the surface or submerge into the center of the droplet, one can study the dynamics of excitation and ionization through the droplet. When resonantly exciting the droplet, we observe a strong ionization enhancement for atoms attached to the surface. On the other hand, atoms embedded inside the nanodroplet are less efficiently ionized. We attribute this effect to an ultrafast energy transfer to the surface of the droplet and subsequent Penning ionization of the surface-bound dopant.

Keywords: free electron laser, XUV laser spectroscopy, atomic, molecular, and cluster physics

(Some figures may appear in colour only in the online journal)

With the development of intense short wavelength sources, such as free electron lasers (FELs) and high harmonic generation sources, one can investigate matter in an entirely new regime and probe nonlinear effects including enhanced multiphoton absorption [1, 2], double core hole states [3, 4] in atoms and molecules, and plasma creation in condensed matter [5, 6]. In particular, clusters and nanodroplets offer a unique intermediate state of matter where both atomic and

condensed matter effects can be observed, such as higher charge state creation compared to atomic states [7], multistep ionization [8], and core state bleaching [9, 10].

Recently, we observed that by irradiating helium nanodroplets with intense resonant XUV light, the ionization rates were almost an order of magnitude larger than those of direct ionization [11] which could not be explained by resonance enhanced multiphoton ionization but rather by an ultrafast interatomic coulombic decay (ICD) [12] leading to a collective autoionization (CAI). From the photoelectron spectra [13], we saw that nearly all excess electron energy

¹² Present address: Istituto di Fotonica e Nanotecnologie CNR-IFN, I-20133 Milano, Italy.

was deposited into the droplet leading to only low energy electron emission and nanoplasma formation. For an overview of research in nanoplasma dynamics, please see the following reviews [14, 15]. The ionization dynamics were explained by the many excited states forming a network where energy is exchanged through either (i) an ICD-type energy exchange followed by inelastic collisions between the ejected electrons and neighboring excited atoms or (ii) a non-sequential process where excited neighbors are ionized by a shake-off like process [13]. In both cases, all excess electron energy is deposited in the droplet leading to the observed low kinetic electron energies. In contrast to prior work on nanoplasma formation (e.g. [7–9]) where the photon energy was above the ionization threshold of the cluster, for CAI, the clusters were first in an excited state and the nanoplasma formed after an ultrafast energy transfer between the excited constituents. As such, the mechanisms and ionization dynamics are still relatively unknown requiring more work on this novel system.

In the present work, we report the first results on the ionization of dopant atoms in He nanodroplets by intense resonant/nonresonant XUV light. We find that the ionization of atoms attached to the surface exhibits a strong dependence on whether the light is on or off resonance with respect to the helium droplet's electronic excitation, while atoms embedded inside the droplet display no such dependence. This effect is attributed to an ultrafast energy transfer towards the surface of the droplet similar to what was observed with synchrotron radiation [16]. However, in stark contrast to the previously mentioned results where multiple excitations were vanishingly rare in the droplet, here the droplets are highly excited due to the much higher power density of the FEL. The decay from this multiply excited state, although estimated to require only a few fs [13], still exhibits a fast migration of excitation to the surface of the droplet.

The experiment was performed at the low density matter beamline [17, 18] at the seeded XUV-FEL, FERMI, which offers wide tunability [19], narrow bandwidth ($\sim 10^{-3}$), and high intensity (up to 10^{14} W cm $^{-2}$) [20]. The photon energy of the FEL was tuned via the seed laser, the undulator gaps, and other machine parameters. The FEL pulse length was estimated to be about 100 fs FWHM with a Gaussian spatial profile of 75 μ m diameter (FWHM) at the focus. The laser pulse energy at the setup is calculated from the value measured upstream on a shot-by-shot basis by gas ionization, taking into account the calculated nominal reflectivity of the optical elements in the beam transport system [18]. The helium droplet beam was produced by supersonic expansion of helium at a backing pressure of 50 bar through a pulsed 50 μ m nozzle which was cryogenically cooled to the low Kelvin range. From these expansion conditions and scaling laws, the droplet size was determined [21], and was experimentally confirmed by titration measurements [22]. The nozzle temperature for this particular experiment was set to 12 K corresponding to an average droplet size of 26 000 He atoms. The droplets were doped using the 'pick-up' process [23] with either a gas doping cell (xenon) or an oven doping cell (lithium). Xenon is known to be located in the bulk of the

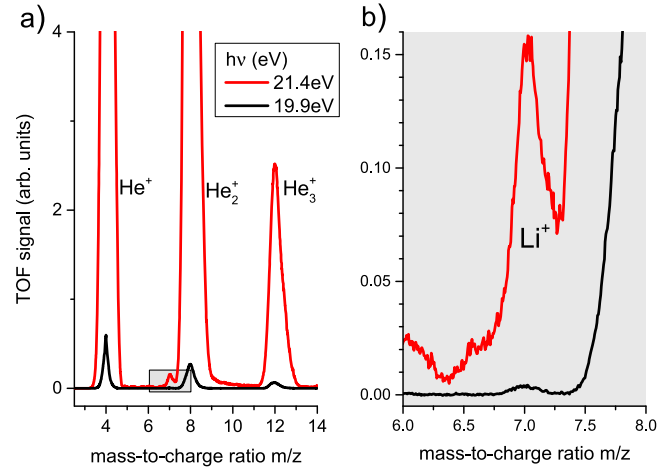


Figure 1. (a) Mass spectra of Li-doped He droplets at $h\nu = 21.4$ eV (red line) and $h\nu = 19.9$ eV (black line). The FEL power is $1.1 \cdot 10^{13}$ W cm $^{-2}$. (b) The same mass spectra as (a) expanded around the Li mass.

He droplet whereas lithium is attached to the surface of the droplet [24, 25]. Thus the different dopants can be an ideal monitor for identifying the role of energy transfer in the ionization process. The lithium oven was set to 450 $^{\circ}$ C corresponding to an average of a single lithium atom being attached to the surface of the droplet, while the partial pressure of the gas pick-up cell was set to 2.5×10^{-3} mbar corresponding to an average of 16 Xe atoms embedded in the nanodroplet. The cluster beam was perpendicularly crossed by the FEL beam at the center of the first acceleration region of a Wiley–McLaren style time-of-flight mass spectrometer (TOF) [26].

Figure 1(a) shows the ion mass spectra for lithium-doped helium nanodroplets irradiated by light of photon energy $h\nu = 21.4$ eV (red line) and $h\nu = 19.9$ eV (black line) with a power density of 1×10^{13} W cm $^{-2}$ for both photon energies. For $h\nu = 21.0$ – 22.3 eV (with a maximum at $h\nu = 21.4$ eV), He nanodroplets exhibit a broad band structure in the absorption spectrum initially observed in early synchrotron radiation work [27]. The strongest band was assigned to the droplet equivalent of the 1s2p atomic transition which was considered broadened by the extended surface region of the cluster and blueshifted due to the repulsive interaction between the excited electron and the neighboring He environment. For energies below $h\nu = 20.5$ eV, no additional excitation levels were observed for He clusters, and the system is therefore considered to be nonresonant.

Comparing resonant to nonresonant ionization, one observes a strong enhancement of the helium oligomer mass peaks due to CAI [11, 13]. Additionally, when resonantly exciting the droplets, a peak appears at $m/z = 7$ due to the ionization of lithium. Figure 1(b) shows the same mass spectra expanded around the lithium peak. Here, one can clearly see that the resonant light strongly enhances the lithium signal as only a small peak is observed when the photon energy is nonresonant for helium. In terms of the enhancement, quantitatively, the lithium signal is about 37 times larger when the helium is resonantly excited compared

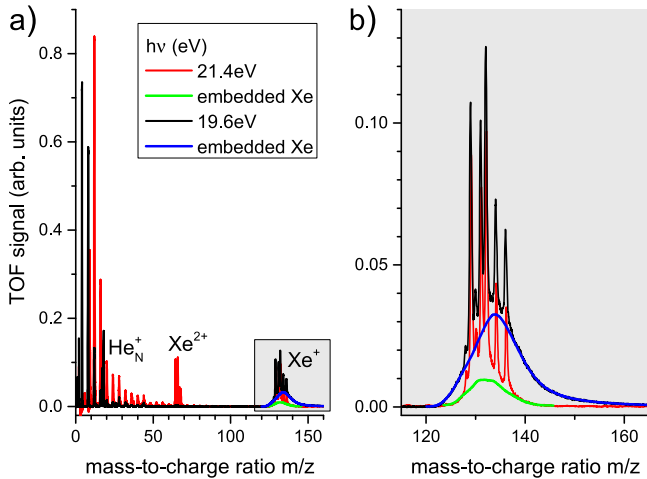


Figure 2. (a) Mass spectra of Xe-doped He droplets at $h\nu = 21.4$ eV (red line) and $h\nu = 19.6$ eV (black line). The FEL power is 1.10^{13} W cm $^{-2}$. (b) The same mass spectra as (a) expanded around the Xe mass. Background-subtracted signal is shown in green ($h\nu = 21.4$ eV) and blue ($h\nu = 19.6$ eV).

to when the photon energy is off resonance at $h\nu = 19.9$ eV. The photoionization cross sections of lithium at $h\nu = 19.9$ eV and 21.4 eV are 0.51 and 0.45 Mbarn [28], respectively. Therefore, there should be little difference in the ionization efficiency for the two photon energies if the lithium atoms were directly ionized and the helium played no role in the ionization process.

Figure 2(a) shows the ion mass spectra for xenon-doped helium nanodroplets with similar experimental conditions to those shown in figure 1 for $h\nu = 21.4$ eV (red line) and 19.6 eV (black line). For $h\nu = 21.4$ eV, the ion TOF electrodes were pulsed using a high voltage switch (Behlke Power Electronics GmbH) to eliminate the large helium monomer signal. Besides that, the progression of helium oligomers is identical to that which is shown in figure 1. The region of the mass spectra from 120 to 160 amu, containing all of the natural isotopes of Xe, is expanded in figure 2(b). The sharp peaks observed in the spectra for both photon energies are due to ionization of atomic xenon that is not attached to helium droplets and reaches the interaction region effusively. The signal from xenon embedded in the droplet (green line for resonant excitation and blue line for nonresonant excitation in figure 2(b)) shows a broad distribution in which the various xenon isotopes are unresolved due to the Coulomb explosion of Xe clusters, similar to previously reported results (e.g. [7]). To distinguish the embedded and effusive Xe signal, a spectrum of purely effusive Xe was taken which was then subtracted from the spectra shown in figure 2(a). Additionally, around mass 65 , doubly ionized xenon is observed in the mass spectra for effusive gas (not embedded in He droplets). The strong enhancement of the Xe^{2+} for $h\nu = 21.4$ eV can be explained by the photon energy being above the second ionization potential of Xe [29]. At this energy, double ionization of xenon is a sequential two photon process, whose second step is resonantly assisted by excitation of the Xe^+ ground state ion to the 1D_2 $6d$ state, followed by autoionization to Xe^{2+} [30]. That being said, no signal of doubly

ionized Xe embedded in the droplet was observed, most likely due to charge transfer between the doubly ionized xenon and the surrounding He atoms.

Xenon shows the opposite trend in comparison to lithium in that when the photon energy corresponds to the helium resonance a reduction of the overall signal is observed. In quantitative terms, the integrated signal of xenon embedded in the nanodroplet is 4.5 times smaller for $h\nu = 21.4$ eV compared to $h\nu = 19.6$ eV. The photoionization cross sections of xenon at $h\nu = 19.6$ eV and 21.4 eV are 38.1 and 29.6 Mbarn [31], respectively. Although the cross-section of xenon at $h\nu = 21.4$ eV is significantly larger than that of lithium in this photon range, the observed Li signal is actually much larger than the Xe signal, signifying that the He environment is instrumental in the ionization process.

To shed light on the present results, one can look at complementary studies using synchrotron radiation to excite/ionize He nanodroplets where a rich spectrum of relaxation processes was observed (e.g. autoionization, emission of slow electrons, charge/excitation migration) [32–34]. In particular, Buchta *et al* [16] observed that when the droplet was electronically excited, the dominating ionization mechanism of surface-bound alkali dopants was a Penning-type ionization while dopants embedded in the center of the droplet showed little to no effect due to helium excitation. On the other hand, when scanning the photon energy, a marked increase in the ion yield was observed for embedded dopants at the ionization threshold of helium. These results were interpreted as due to a charge transfer process between the He ion and the dopant, indicating fast exciton as well as positive hole migration in the droplet [35].

Here, we propose a simple model to explain the observed phenomena, which is schematically shown in figures 3 and 4. Figure 3 shows the case where the radiation is off resonance with respect to the nanodroplet for (a) Li-doped droplets ($h\nu = 19.9$ eV) and (b) Xe-doped droplets. For each case, the ionization of the He environment must proceed through a two photon ionization process or second harmonic FEL radiation leading to only a few ionized atoms due to the small ionization cross section. For lithium (figure 3(a)), direct ionization is not likely due to the low ionization cross section (0.51 Mbarn) at high photon energies. Furthermore, since the probability of He ionization is also weak, we do not expect substantial signal of Li^+ ions by charge transfer ionization. Therefore, there is relatively little Li^+ observed in the mass spectra shown in figure 1. For xenon (figure 3(b)), the helium droplet remains relatively unaffected by the FEL radiation similar to the case of Li. In contrast to Li-doped droplets, xenon has a high ionization cross section (36.1 Mbarn) and therefore can be directly ionized leading to the larger Xe signal observed in the mass spectra in figure 2.

Figure 4 shows the case where the radiation is on resonance with respect to the nanodroplet ($h\nu = 21.4$ eV) for (a) Li-doped droplets and (b) Xe-doped droplets. In this case, when the doped droplets are irradiated by resonant light ($h\nu = 21.4$ eV), the situation is completely different. Within the first 50 fs of the FEL pulse, about 50% of the droplet is excited, schematically shown as the red double-lobe

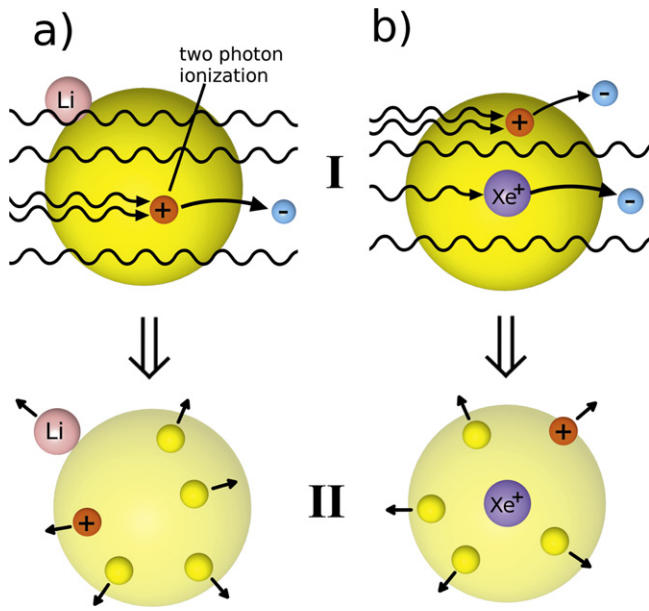


Figure 3. Schematic representation of the dopant ionization process when the He droplet is not resonantly excited ($h\nu = 19.9$ eV for (a) Li and $h\nu = 19.6$ eV for (b) Xe). (I) The helium droplet is weakly ionized by a two photon processes leading to (II) expansion and fragmentation. Due to the low cross section, Li is unlikely to be directly ionized whereas the large cross section for Xe makes direct ionization more likely.

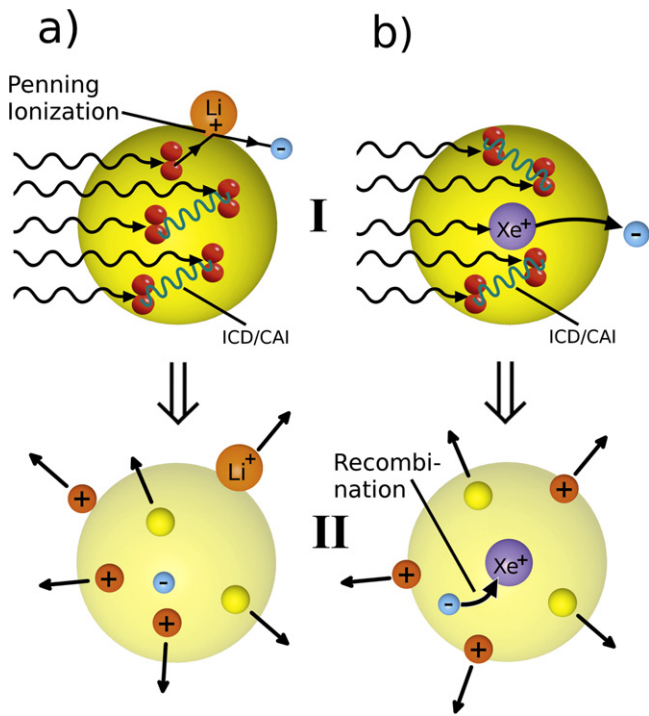


Figure 4. Schematic representation of the dopant ionization process when the He droplet is resonantly excited ($h\nu = 21.4$ eV) for (a) Li and (b) Xe. (I) The droplet is excited leading to collective autoionization and Penning ionization for the attached Li (I a). (II) A nanoplasma is formed leading to Coulomb explosion while the Xe^+ recombines with electrons in the formed nanoplasma (II b).

distribution in figure 4. As previously reported [11, 13], such an environment leads to a CAI process followed by nanoplasma formation in the droplet.

For Li-doped droplets, shown in figure 4(a), a clear enhancement is observed due to resonant excitation of the He environment. The question which immediately arises is which process is responsible for this effect. As mentioned, the excited He atoms can Penning ionize the attached atom(s) [16]. Furthermore, from merged beam experiments, it was shown that the Penning ionization cross section for $He^*(1s2s)-He^*(1s2s)$ and $He^*(1s2s)-Li$ were quantitatively equivalent [36]. In the present case, one would therefore expect that Penning ionization of the attached lithium atom would be as likely as CAI when an excited helium is nearby. Additionally, the ionization process is considered to be ultrafast with a lifetime in the range of tens to hundreds of fs [12]. After CAI, a nanoplasma is formed opening additional ionization pathways such as electron impact and field ionization [37]. As Penning ionization precedes nanoplasma formation, it is the most likely ionization mechanism while the droplet is in the excited state, however, ionization in the nanoplasma cannot be neglected. As such, one can make some simple estimates of the probability of electron impact ionization and surface field ionization [15] assuming a Gaussian FEL beam for the experimental parameters given above. For 50% of the droplets which absorbed a minimum of one photon, field ionization of lithium is possible while the average probability for electron impact ionization of Li is 3.2%.

The interpretation of the ultrafast surface migration is additionally supported by pump-probe results for singly-excited nanodroplets [38] where high lying Rydberg states were shown to relax energetically within a few hundred fs. Kornilov *et al* [38] used a simple model which gave good agreement with experimental data to explain these effects by treating the excitation as localized at a single atom within the droplet which is then perturbed by the mean field of the surrounding He atoms. The excited atom moves to the surface due to the change in density of the surrounding He environment. Recently, similar results were observed for excitation of the 2p band in He droplets where surface migration was observed to occur within 400 fs [39].

In contrast to lithium, when the droplet is resonantly excited, the Xe signal shown in figure 1 decreases compared to the nonresonant case. The ionization mechanism explaining the lower signal is shown in figure 4(b). Initially, the Xe atom(s) are directly ionized along with the He environment which is collectively excited. The excited helium then undergoes CAI leading to nanoplasma formation on the surface of the droplet. Additionally, after CAI, charge transfer ionization of Xe is also possible [16]. The resulting shell of ions then undergoes Coulomb explosion/hydrodynamic expansion while excess electrons can recombine with ions in the center of the droplet. In comparison to IR-induced nanoplasma formation of Xe-doped nanodroplets [40–42]

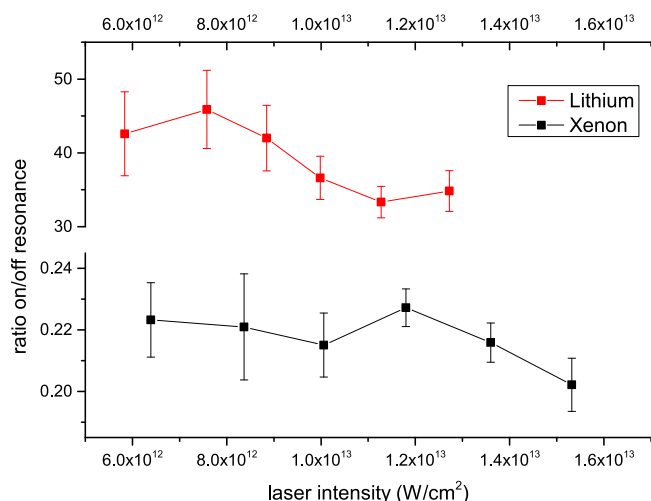


Figure 5. Ratio of dopant ions for on and off resonant droplet excitation as a function of the FEL power for lithium (top) and xenon (bottom).

where the Xe atoms trigger the nanoplasma formation and the dynamics are mediated by the strong coupling between the radiation and electrons from ionized xenon, here, the excited He atoms form a nanoplasma while the Xe atoms essentially play the role of a spectator in the process.

Figure 5 shows the ratio of dopant ions measured for on and off resonant droplet excitation as a function of the FEL intensity for lithium (top) and xenon (bottom). The nozzle temperature and number of attached atoms are the same as described in figures 1 and 2. For both cases, the on/off resonance ratio remains relatively unchanged over the entire measured FEL power range.

For the case of xenon, the results are not surprising and fit our proposed model. For both photon energies, the embedded xenon atoms are directly ionized by a single photon and, therefore, both power dependencies should be linear. Therefore, their ratio should remain unchanged with respect to the laser power. A ratio less than one is explained by the process described in figure 4(b) where the excess electrons created during the nanoplasma formation recombine with the Xe ions resulting in a lower measured Xe signal.

For Li-doped droplets, at $h\nu = 19.9$ eV, the attached lithium atoms are directly, though weakly, ionized by a single photon while, at $h\nu = 21.4$ eV, ionization primarily occurs through a Penning process with an excited He atom. As He excitation is also a single photon process, the resonant/non-resonant ratio remains constant with respect to laser power. A ratio much greater than one is understood by the high efficiency of Penning ionization compared to direct ionization of lithium.

In conclusion, a strong enhancement in the ionization of Li atoms attached to the surface of He droplets was observed when the He environment was resonantly excited by intense FEL radiation. In contrast, a decrease in the ionization of Xe atoms embedded in the center of droplets was observed for the same conditions. The process is explained by the excited He atoms migrating to the surface of the droplet where Li is

ionized in a Penning process while the Xe ions recombine with the excess electrons created during nanoplasma formation.

Acknowledgments

We would like to thank U Saalman, A Heidenreich, R Richter, and T Fennel for their enlightening discussions on this subject and gratefully acknowledge the support of the entire FERMI team.

References

- [1] Richter M et al 2009 *Phys. Rev. Lett.* **102** 163002
- [2] Young L et al 2010 *Nature* **466** 56
- [3] Berrah N et al 2011 *Proc. Natl Acad. Sci. USA* **108** 16912
- [4] Nakano M et al 2013 *Phys. Rev. Lett.* **110** 163001
- [5] Vinko S et al 2012 *Nature* **482** 59
- [6] Nagler B et al 2009 *Nat. Phys.* **5** 693
- [7] Wabnitz H et al 2002 *Nature* **420** 482
- [8] Bostedt C et al 2008 *Phys. Rev. Lett.* **100** 133401
- [9] Schorb S et al 2012 *Phys. Rev. Lett.* **108** 233401
- [10] Saalman U and Rost J-M 2002 *Phys. Rev. Lett.* **89** 143401
- [11] LaForge A et al 2014 *Sci. Rep.* **4** 3621
- [12] Kuleff A I, Gokhberg K, Kopelke S and Cederbaum L S 2010 *Phys. Rev. Lett.* **105** 043004
- [13] Ovcharenko Y et al 2014 *Phys. Rev. Lett.* **112** 073401
- [14] Saalman U, Siedschlag C and Rost J 2006 *J. Phys. B: At. Mol. Opt. Phys.* **39** R39
- [15] Fennel T et al 2010 *Rev. Mod. Phys.* **82** 1793
- [16] Buchta D et al 2013 *J. Phys. Chem. A* **117** 4394
- [17] Lyamayev V et al 2013 *J. Phys. B: At. Mol. Opt. Phys.* **46** 164007
- [18] Svetina C et al 2015 *J. Synchrotron Radiat.* **22** 538
- [19] Allaria E et al 2012 *New J. Phys.* **14** 113009
- [20] Allaria E et al 2012 *Nat. Photonics* **6** 699
- [21] Hagena O and Obert W 1972 *J. Chem. Phys.* **56** 1793
- [22] Gomez L F, Loginov E, Sliter R and Vilesov A F 2011 *J. Chem. Phys.* **135** 154201
- [23] Gough T, Mengel M, Rowntree P and Scoles G 1985 *J. Chem. Phys.* **83** 4958
- [24] Toennies J P and Vilesov A F 2004 *Angew. Chem., Int. Ed. Engl.* **43** 2622
- [25] Stienkemeier F et al 1996 *Z. Phys. D: At. Mol. Clusters* **38** 253
- [26] Wiley W and McLaren I H 1955 *Rev. Sci. Instrum.* **26** 1150
- [27] Joppin M, Karnbach R and Möller T 1993 *Phys. Rev. Lett.* **71** 2654
- [28] Hofsaess D 1977 *Z. Phys. A: Hadrons Nucl.* **281** 1
- [29] Kramida A, Ralchenko Yu, Reader J and NIST ASD Team 2014 *NIST Atomic Spectra Database version 5.2* (Gaithersburg, MD: National Institute of Standards and Technology) (<http://physics.nist.gov/asd>)
- [30] Bizau J M et al 2011 *J. Phys. B: At., Mol. Opt. Phys.* **44** 055205
- [31] Samson J and Stolte W C 2002 *J. Electron Spectrosc. Relat. Phenom.* **123** 265
- [32] Fröchtenicht R et al 1996 *J. Chem. Phys.* **104** 2548
- [33] Peterka D S, Lindinger A, Poisson L, Ahmed M and Neumark D M 2003 *Phys. Rev. Lett.* **91** 043401
- [34] von Haefen K, Laarmann T, Wabnitz H and Möller T 2005 *J. Phys. B: At. Mol. Opt. Phys.* **38** S373
- [35] Buchenau H, Toennies J and Northby J 1991 *J. Chem. Phys.* **95** 8134
- [36] Wang D, Tang S and Neynaber R 1987 *J. Phys. B: At. Mol. Opt. Phys.* **20** 1527

- [37] Gnodtke C, Saalmann U and Rost J M 2009 *Phys. Rev. A* **79** 041201
- [38] Kornilov O *et al* 2011 *J. Phys. Chem. A* **115** 7891
- [39] Ciavardini A *et al* 2015 to be published
- [40] Mikaberidze A, Saalmann U and Rost J M 2009 *Phys. Rev. Lett.* **102** 128102
- [41] Döppner *et al* 2010 *Phys. Rev. Lett.* **105** 053401
- [42] Krishnan S R *et al* 2011 *Phys. Rev. Lett.* **107** 173402